

Title	Importance of interstory velocity on optimal along-height allocation of viscous oil dampers in super high-rise buildings
Author(s)	Adachi, Fuyuki; Fujita, Kohei; Tsuji, Masaaki; Takewaki, Izuru
Citation	Engineering Structures (2013), 56: 489-500
Issue Date	2013-11
URL	http://hdl.handle.net/2433/176339
Right	© 2013 Elsevier B.V.
Type	Journal Article
Textversion	author

Importance of interstory velocity on optimal along-height allocation of viscous oil dampers in super high-rise buildings

Fuyuki Adachi, Kohei Fujita, Masaaki Tsuji and Izuru Takewaki*

Department of Architecture and Architectural Engineering, Kyoto University,
Kyotodaigaku-Katsura, Nishikyo-ku, Kyoto 615-8540, Japan,

*Corresponding author: takewaki@archi.kyoto-u.ac.jp

ABSTRACT

The effective way of allocation of viscous oil dampers (capacity or size) is believed to place dampers to the stories which exhibit large interstory drifts. It is shown here that, while this understanding is almost true in rather low or medium-rise buildings, the distribution of the maximum interstory velocities plays a critical role in super high-rise buildings. It is further demonstrated that a large distribution of the maximum interstory velocities can be observed in lower stories in super high-rise buildings and this leads to a large demand of the maximum damping force in lower stories. It is concluded that the demand of relief forces of oil dampers is expressed in terms of (a) the maximum story shear forces of a frame without oil dampers which can be evaluated by the response spectrum method or other conventional methods, (b) the damper damping ratio, (c) the damping correction factor and (d) the higher-mode correction factor.

Keywords: Viscous damper, super high-rise building, damper effectiveness, demand of relief force, interstory velocity, unexpected property

1. Introduction

There are a variety of passive dampers for building structures under earthquake ground motions [1-4]. Hysteretic steel dampers (shear deformation type, buckling restrained type), viscous wall-type dampers, viscous oil dampers, visco-elastic dampers, friction dampers are representative ones. Recently viscous oil dampers (called oil dampers hereafter) are often used from the viewpoints of stable mechanical properties, low frequency and temperature dependencies and cost effectiveness, etc. together with hysteretic steel dampers.

Many research works have been accumulated so far on the damper optimization [4-17], i.e. damper size and location. While most of them deal with linear responses, quite a few treat non-linear responses in building structures or dampers [11, 18, 19]. However, there is no research except [20] on the optimization of location and quantity of dampers which deals

directly with non-linear responses and includes simple and systematic algorithms. Although simple and systematic algorithms for damper optimization are useful in research, more simplified procedures are desired in the usual structural design practice.

The purpose of this paper is to demonstrate that the distribution of the maximum interstory velocities is a key index for evaluating the along-height effectiveness and demand of viscous-type oil dampers and its distribution exhibits special characteristics depending on the number of stories of building frames to be considered. A simplified evaluation procedure of the demand of oil dampers is also presented. It will be shown that the demand of relief forces of oil dampers is expressed in terms of (a) the maximum story shear forces of a frame without oil dampers which can be evaluated by the response spectrum method or other conventional methods, (b) the damper damping ratio, (c) the damping correction factor and (d) the higher-mode correction factor.

Most structural engineers seek for the design procedure to evaluate the required damper capacity (damping coefficient and relief force in the case of viscous oil dampers) directly from the frame response without dampers. Since the existence of two parameters, damping coefficient and relief force, seems to cause a difficulty in investigating the simplified design method for oil dampers, the distribution of damping coefficients is limited to a frame stiffness proportional one. It is also well known that the capacity of oil dampers depends mainly on the relief force (or the limiting damping force) and not on the damping coefficient [20]. It is pointed out in this paper that special characteristics on the effective location and demand of viscous oil dampers can be observed especially in super high-rise buildings and these characteristics can be explained by paying attention to the distribution of the maximum interstory velocities, not the distribution of the maximum interstory drifts.

Once the required linear damper capacity is obtained, it is known [20, 21] that the specification of the reduction ratio of the relief force from the corresponding linear damping force is possible so as not to change the displacement response of building frames including dampers with the relief mechanism from that of building frames including linear dampers.

2. Frame including oil dampers with relief mechanism

Consider oil dampers with a relief mechanism [20, 21] and a planar frame model with those oil dampers. The damping force - velocity relation of the oil damper is shown in Fig.1.

Let $c_{1j,i}$ denote the damping coefficient of the oil damper in the j -th story and i -th span under the relief force and $c_{2j,i}$ denote that beyond the relief force. The relief force and the angle of the oil damper from the horizontal line are denoted by $d_{Rj,i}$ and $\phi_{j,i}$, respectively. The ratio of $c_{2j,i}$ to $c_{1j,i}$ is usually specified as 0.05-0.10. Let $f_{j,i\max}$ denote the maximum damping force of the oil damper in the j -th story and i -th span and let $f_{Lj,i\max}$ denote the maximum damping force of the ‘linear oil damper’ in the j -th story and i -th span. The ratio of $d_{Rj,i}$ to $f_{Lj,i\max}$ is called ‘the damping force limit ratio’ and is defined by

$$L_{j,i} = \frac{d_{Rj,i}}{f_{Lj,i\max}} \quad (1)$$

This damping force limit ratio plays an important role in the design of oil dampers. From Eq.(1), the relief force can be expressed in terms of the damping force limit ratio $L_{j,i}$ and the maximum damping force $f_{Lj,i\max}$ of the linear oil damper.

$$d_{Rj,i} = L_{j,i} f_{Lj,i \max} \quad (2)$$

It is well recognized [20, 21] that, when 0.5-1.0 is employed as $L_{j,i}$, the frame including the oil dampers with the relief mechanism exhibits almost the same performance (horizontal displacement, etc.) as the frame including the oil dampers without the relief mechanism, i.e. linear oil dampers.

Because it is well known that, when a sufficient supporting member stiffness is used, the viscous oil damper exhibits a sufficient performance with respect to its relative velocity of member ends [22], it is assumed here that the oil damper shows the complete performance with its relative velocity of both member ends including the supporting members.

3. Prediction of maximum damping force of linear oil damper from story shear force in frame without oil damper

In the field of structural control by passive dampers, the ratio of the force sustained by passive dampers to the total story shear force (or the story shear force at the main frame) is a good measure of the effect of passive dampers. It is therefore reasonable to relate the force sustained by passive dampers to the total story shear force. The approximation of the maximum interstory velocity in terms of the maximum interstory drift (harmonic vibration approximation) makes it possible to express the maximum damping force in terms of the maximum interstory drift. The following formulation is based on this concept.

Let $\omega^{(1)}$ and $\delta_{ff \max}$ denote the fundamental natural circular frequency and the maximum interstory drift in the j -th story of the frame without oil dampers. Assume that the maximum interstory velocity can be evaluated approximately by $\omega^{(1)} \delta_{ff \max}$. Then the maximum damping force $f_{Lj,i \max}$ of the linear oil damper may be predicted by

$$f_{Lj \max} = c_{1j} \omega^{(1)} \delta_{ff \max} \quad (3)$$

Although the maximum interstory drift of the frame without oil dampers may be different from that of the frame with oil dampers, the influence will be considered later. The damping coefficient with respect to the horizontal direction of an oil damper is assumed to be proportional to the frame story stiffness k_{ff} . This leads to

$$c_{1j} = \frac{2h_d^{(1)}}{\omega^{(1)}} k_{ff} \quad (4)$$

where $h_d^{(1)}$ is the lowest-mode damping ratio of oil dampers. The present paper is aimed at discussing the demand of the maximum damping forces of oil dampers. While the damper damping coefficients may be related indirectly to these maximum damping forces, it seems that the relief forces are related directly to these maximum damping forces.

Substitution of Eq.(4) into Eq.(3) provides

$$f_{Lj \max} = 2h_d^{(1)} k_{ff} \delta_{ff \max} \quad (5)$$

The story shear force $Q_{ff \max}$ of the building frame without oil dampers can be expressed approximately as $Q_{ff \max} = k_{ff} \delta_{ff \max}$. Then Eq.(5) leads to

$$f_{Lj\max} = 2h_d^{(1)}Q_{ff\max} \quad (6)$$

4. Numerical examples

4-1 Frame model and input ground motion

Consider 10-story, 20-story, 40-story and 60-story steel building frames. 10 and 20-story frames have three spans and 40 and 60-story frames have 5 spans. The geometrical properties and the fundamental natural periods of these frames are shown in Fig.2. The member cross-sectional properties are presented in Tables 1(a), 2(a), 3(a), 4(a). It is assumed in the present numerical examples that two oil dampers are placed in the middle span as shown in Fig.2. The structural damping matrix of the main frame is assumed to be proportional to the stiffness matrix and is given by

$$\mathbf{C}_s = \frac{2h_s^{(1)}}{\omega^{(1)}} \mathbf{K} \quad , \quad h_s^{(1)} = 0.02 \quad (7)$$

where $h_s^{(1)}$ is the lowest-mode structural damping ratio of the main frame. In Eqs.(4, 5), the story stiffness k_{ff} is to be evaluated by the following equation in which $\omega^{(1)}$ and $u_i^{(1)}$ are the fundamental natural circular frequency and the lowest eigenmode of the frame model and N denotes the number of stories of the frame.

$$k_{ff} = \omega^{(1)2} \frac{\sum_{i=j}^N m_i u_i^{(1)}}{u_j^{(1)} - u_{j-1}^{(1)}} \quad (u_0^{(1)} = 0; j = 1, 2, \dots, N) \quad (8)$$

In Eq.(8), N is the number of stories. This is an inverse problem in which a set of story stiffnesses is determined from the lowest eigenpair of the fundamental natural circular frequency and the lowest eigenmode. The damper damping coefficient with respect to the axial direction can be evaluated by

$$c_{1j,i} = \frac{c_{1j}}{2 \cos^2 \phi_{j,i}} \quad (9)$$

This value is shown in Tables 1(b), 2(b), 3(b), 4(b) together with k_{ff} in Eq.(8).

Fig.3 shows the ratio of the shear deformation to the interstory drift in a building frame with three damper levels ($h_d^{(1)} = 0.05, 0.10, 0.15$). The shear deformation can be evaluated by extracting the bending-deformation component shown in Fig.4 from the total interstory drift.

The damping ratio can be specified by structural designers. The structural designers usually determine the damping ratio judging from the target response at which the structural designers aim. For example, once the target response (e.g. maximum interstory drift) is specified, the lowest-mode damping ratio of linear oil dampers can be obtained through a few numerical investigations. After the lowest-mode damping ratio of linear oil dampers is obtained, the damping force limit ratio (0.5-1.0) can be used to determine the relief forces of

oil dampers.

El Centro NS 1940, Taft EW 1952 and Hachinohe NS 1968 with the maximum ground velocity of 0.5(m/s) are used as the input ground motions. This level is called ‘Level 2 (Lv.2)’ in Japan for structural design of super high-rise buildings. Because similar tendencies were observed for these three ground motions, only the result for El Centro NS 1940 will be shown in Sections 4-2, 4-3, 4-4. The frequency contents of earthquake ground motions affect the vibration modes amplified during earthquakes. In the conventional (ordinary) ground motions, higher modes are somewhat amplified in high-rise buildings. This phenomenon is treated in the present paper. However, in long-period ground motions which are controversial in Japan, higher modes may not be influential in high-rise buildings.

4-2 Maximum horizontal damping force $f_{Lj\max}$ in linear oil damper and its approximate prediction $2h_d^{(1)}Q_{ff\max}$

The maximum horizontal damping force $f_{Lj\max}$ of both linear oil dampers in the j -th story can be obtained from the maximum damping force $f_{Lj,i\max}$ of one linear oil damper in the j -th story.

$$f_{Lj\max} = 2f_{Lj,i\max} \cos \phi_{j,i} \quad (10)$$

Fig.5 shows the maximum horizontal damping force $f_{Lj\max}$ in the linear oil damper and its approximate prediction $2h_d^{(1)}Q_{ff\max}$. While a fairly good correspondence can be seen in the 10-story frame, it is also understood that a correction should be made in other frames of different number of stories (20, 40, 60-story) depending on the damper level. Amplification of damping force in lower stories should also be amended.

4-3 Maximum interstory drift and maximum interstory velocity of building frame with linear oil damper

In order to examine the influence of the maximum interstory drifts and the maximum interstory velocities on the maximum horizontal damping force of oil dampers, those quantities have been computed for frames without oil dampers and those with 15% linear damping.

Fig.6 illustrates the maximum interstory drift and maximum interstory velocity of building frames without and with linear oil dampers. It is observed that a peculiarly large interstory velocity can be seen in lower stories in 40 and 60-story frames.

Fig.7 shows the absolute distribution of the interstory eigenmode of the building frame without oil dampers multiplied by its participation factor. It can be concluded that the superposition of interstory-drift eigenmodes in lower stories is the main reason of the amplification of the maximum interstory velocities in lower stories in 40 and 60-story frames. This greatly influences the along-height effectiveness of oil dampers in super high-rise building frames.

Super high-rise buildings can be modeled by a cantilever beam with ‘shear deformation’. Even if a building becomes taller, the deformation in lower stories are governed by shear deformation and bending deformation. For comparison purpose, a cantilever beam without shear deformation has been analyzed for a 60-story frame. Fig.A1(a) in appendix shows the participation vector for the first four eigenmodes and Fig.A1(b) illustrates the absolute values of interstory drift participation vectors for the first four eigenmodes. Fig.A1(b) corresponds to Fig.7(d). Usual oil dampers are effective only for shear deformation, not bending

deformation. Although a cantilever beam without shear deformation can be analyzed rather easily using a continuum theory as shown above, the cantilever with shear deformation cannot be analyzed easily to the best of the authors' knowledge. The ratio of shear deformation to bending deformation depends on the story level. In lower stories, the ratio of shear deformation to bending one is large. In addition, usual building frames have a large difference of story stiffnesses in the lower stories and the upper stories as seen from Tables 1(b), 2(b), 3(b), 4(b). These indicate that, while a continuum approach based on the model with constant cross-section provides some interesting results, careful analysis and evaluation of the results are necessary.

4-4 Maximum horizontal damping force $f_{Lj\max}$ in linear oil damper and its approximate prediction $Z(2h_d^{(1)}Q_{ff\max})$ in terms of damping correction factor Z

Because it was made clear that the damping level of oil dampers is a key parameter for correcting the relation between the maximum horizontal damping force $f_{Lj\max}$ in the linear oil damper and its approximate prediction $2h_d^{(1)}Q_{ff\max}$, the following coefficient Z is introduced.

$$f_{Lj\max} = Z(2h_d^{(1)}Q_{ff\max}) \quad (11)$$

where

$$Z = -0.2Nh_d^{(1)} + 1.2 \quad \text{for } N=10 \text{ and } 20 \quad (12)$$

$$Z = 1 \quad \text{for } N=40 \text{ and } 60 \quad (13)$$

Fig.8 shows the maximum horizontal damping force $f_{Lj\max}$ in linear oil dampers and its approximate prediction $Z(2h_d^{(1)}Q_{ff\max})$ (El Centro NS 1940 (Lv.2)). The influence of damping level has been included appropriately. However the amplification of the maximum horizontal damping force in lower stories is not yet reflected in super high-rise buildings.

4-5 Maximum horizontal damping force $f_{Lj\max}$ in linear oil damper and its approximate prediction $Y_j\{Z(2h_d^{(1)}Q_{ff\max})\}$ in terms of damping correction factor Z and higher-mode correction factor Y_j

In order to amend the amplification of the maximum horizontal damping force in lower stories, a new coefficient Y_j is introduced for 20, 40 and 60-story frames. This correction is made only for high-rise buildings, i.e. $Y_j = 1 (j=1, \dots, N)$ for 10-story frames. This coefficient is a fourth-order polynomial function of height (story number j) which is expressed by

$$Y_j = C_1j^4 + C_2j^3 + C_3j^2 + C_4j + C_5 \quad (j=1, 2, \dots, N/2 : N = \text{number of stories}) \quad (14)$$

The coefficients Z and Y_j are summarized as follows.

$$f_{Lj\max} = Y_j\{Z(2h_d^{(1)}Q_{ff\max})\} \quad (15)$$

$$Z = \begin{cases} -0.2Nh_d^{(1)} + 1.2 & N = 10, 20 \\ 1 & N = 40, 60 \end{cases} \quad (16)$$

($N = 10$)

$$Y_j = 1 \quad j = 1, 2, \dots, N \quad (17a)$$

($N = 20, 40, 60$)

$$Y_j = \begin{cases} C_1 j^4 + C_2 j^3 + C_3 j^2 + C_4 j + C_5 & j = 1, 2, \dots, N/2 \\ 1 & j = N/2, N/2 + 1, \dots, N \end{cases} \quad (17b)$$

The coefficients C_1, \dots, C_5 for three damper levels have been obtained by the least-squares procedure for El Centro NS 1940, Taft EW 1952 and Hachinohe NS 1968 with the maximum ground velocity of 0.5(m/s). The mean values of the coefficients for these three ground motions are shown in Table 5 and used in the comparison with the maximum horizontal damping force $f_{Lj \max}$ in the linear oil damper under these three ground motions. It can be summarized that, in low and medium-rise buildings, the effect of higher modes on responses (interstory drift, interstory velocity) is smaller than high-rise buildings. This fact can also be observed from Eq.(17), i.e. the amplification due to higher-mode effect is not seen in 10-story buildings.

Fig.9 shows the maximum horizontal damping force $f_{Lj \max}$ in the linear oil damper and its approximate prediction $Y_j\{Z(2h_d^{(1)}Q_{ff \max})\}$ under El Centro NS 1940 (Lv.2). Fig.10 illustrates the maximum horizontal damping force $f_{Lj \max}$ in the linear oil damper and its approximate prediction $Y_j\{Z(2h_d^{(1)}Q_{ff \max})\}$ under Taft EW 1952 (Lv.2). Fig.11 presents the maximum horizontal damping force $f_{Lj \max}$ in the linear oil damper and its approximate prediction $Y_j\{Z(2h_d^{(1)}Q_{ff \max})\}$ under Hachinohe NS 1968 (Lv.2). It can be observed that the approximate prediction $Y_j\{Z(2h_d^{(1)}Q_{ff \max})\}$ with the appropriate coefficients Y_j provides a reasonable accuracy on the maximum horizontal damping force $f_{Lj \max}$ in the linear oil damper under representative three recorded ground motions except the 20-story frame under Hachinohe NS 1968 (Lv.2). The fundamental natural period 2.49s of the 20-story frame is close to the predominant period of Hachinohe NS 1968 (Lv.2). Therefore the response amplification in this case is quite large especially in the frame with a small damping (i.e. without oil dampers). The damping correction factor Z given by Eqs.(12, 13) should be revised in such a case.

Fig.12 presents the comparison among $f_{Lj \max}$ in linear oil damper and its approximate predictions $Y_j\{Z(2h_d^{(1)}Q_{ff \max})\}$ and $Y_j\{Z^*(2h_d^{(1)}Q_{ff \max})\}$. The revised damping correction factor Z^* is given by

$$Z^* = 0.5Z = 0.5(-0.2Nh_d^{(1)} + 1.2) \quad (18)$$

This correction has been made based on the amplification at 2.49s in the displacement and acceleration response spectra for damping ratios 0.02 and 0.07 for Hachinohe NS 1968 (Lv.2). This is because the normalization of Z has been made for the added damping ratio of 0.05. It can be seen that this revision is acceptable.

The flowchart for evaluation of the demand relief forces of oil dampers is shown in

Fig.13. As stated before, once the demand linear damper capacity (maximum damping force) is obtained, it is known [20, 21] that the specification of the reduction ratio, i.e. 0.5-1.0, of the relief force from the corresponding linear damping force is possible so as not to change the response of building frames including dampers with the relief mechanism from that of building frames including linear dampers. From the economical point of view, the reduction factor 0.5 is recommended.

As for the effect of properties of frames on the correction measures, there are various properties of frames and it seems difficult to derive certain conclusions.

4-6 Effect of frame yielding and concentrated damper allocation

The consideration of yielding of frame members may lead to the amplification of interstory drift and interstory velocity. This may also yield to the amplification of the demand of the maximum damping force of linear oil dampers and the relief forces of oil dampers [23]. A more detailed investigation is necessary for clarifying the relation between yielding of frame members and oil damper demand.

A method for finding the optimal allocation (determination of relief force) of oil dampers has been proposed in the reference [20]. As a result, oil dampers are optimally located at lower stories and upper stories. In the reference [20], the reason was not clear. It seems that one of the reasons has been made clear in the present paper (Section 4-5).

5. Conclusions

The following conclusions have been obtained.

- (1) While it is widely believed that the effective way of allocation of viscous oil dampers is to place dampers to the stories which exhibit large interstory drifts, this applies only to rather low-rise or medium-rise buildings and the distribution of the maximum interstory velocities plays an important and key role in super high-rise buildings.
- (2) An unexpectedly large distribution of the maximum interstory velocities can be observed in lower stories in super high-rise buildings and this fact influences greatly the effective location of viscous oil dampers.
- (3) It has been shown that the demand of relief forces of oil dampers is expressed in terms of (a) the maximum story shear forces of a frame without oil dampers which can be evaluated by the response spectrum method or other conventional methods, (b) the damper damping ratio, (c) the damping correction factor Z and (d) the higher-mode correction factor Y_j . The damping correction factor should be revised when a situation similar to resonance occurs.

The oil damper is being used as an effective tool for retrofitting the super high-rise building especially for long-period ground motions [24-29]. It is expected that the proposed along-height effectiveness will provide a useful design guideline for retrofitting.

Acknowledgments

Part of the present work is supported by the Grant-in-Aid for Scientific Research of Japan Society for the Promotion of Science (No.24246095). This support is greatly appreciated.

Appendix: Reference continuum model without shear deformation

In order to compare with the corresponding continuum model, a bending beam without

shear deformation is analyzed. A 60-story frame model is taken as a comparison model (fundamental natural period=7.19s, height=240m). Fig.A1(a) shows the participation vectors for the first four eigenmodes and Fig.A1(b) illustrates the absolute values of interstory participation vectors for the first four eigenmodes. Fig.A1(b) corresponds to Fig.7(d) for a frame model. It can be observed that, although the height-wise variation of cross-section (story stiffness) and shear deformation are not considered here, Fig.A1(b) exhibits a tendency similar to Fig.7(d) for a 60-story frame.

References

- [1] Soong TT and Dargush GF. Passive energy dissipation systems in structural engineering. John Wiley & Sons, Chichester, 1997.
- [2] Hanson RD and Soong TT. Seismic design with supplemental energy dissipation devices. EERI, Oakland, CA, 2001.
- [3] de Silva CW (ed.). Vibration damping, control, and design. CRC Press, 2007.
- [4] Takewaki I. Building control with passive dampers: -Optimal performance-based design for earthquakes-. John Wiley & Sons Ltd. (Asia), 2009.
- [5] Zhang RH and Soong TT. Seismic design of viscoelastic dampers for structural applications. J Struct Engrg, ASCE 1992; 118: 1375-1392.
- [6] Tsuji M and Nakamura T. Optimum viscous dampers for stiffness design of shear buildings. J Structural Design of Tall Buildings 1996; 5: 217-234.
- [7] Takewaki I. Optimal damper placement for minimum transfer functions. Earthq Engrg Struct Dyn 1997; 26: 1113-1124.
- [8] Takewaki I. Optimal damper placement for planar building frames using transfer functions, Structural and Multidisciplinary Optimization 2000; 20(4): 280-287.
- [9] Garcia DL. A simple method for the design of optimal damper configurations in MDOF structures. Earthquake Spectra 2001; 17: 387-398.
- [10] Singh MP and Moreschi LM. Optimal seismic response control with dampers. Earthq Engrg Struct Dyn 2001; 30: 553-572.
- [11] Uetani K, Tsuji M and Takewaki I. Application of optimum design method to practical building frames with viscous dampers and hysteretic dampers. Engineering Structures 2003; 25: 579-592.
- [12] Liu W, Tong M and Lee G. Optimization methodology for damper configuration based on building performance indices. J Struct Engrg, ASCE 2005; 131(11): 1746-1756.
- [13] Lavan O and Levy R. Optimal design of supplemental viscous dampers for linear framed structures. Earthq Engrg Struct Dyn 2006; 35: 337-356.
- [14] Silvestri S and Trombetti T. Physical and numerical approaches for the optimal insertion of seismic viscous dampers in shear-type structures, J Earthquake Engineering 2007; 11: 787-828.
- [15] Aydin E, Boduroglu MH and Guney D. Optimal damper distribution for seismic rehabilitation of planar building structures. Engineering Structures 2007; 29: 176-185.
- [16] Cimellaro GP. Simultaneous stiffness-damping optimization of structures with respect to acceleration, displacement and base shear. Engineering Structures 2007; 29: 2853-2870.
- [17] Levy R. and Lavan O. Fully stressed design of passive controllers in framed structures for seismic loadings. J Structural and Multidisciplinary Optimization 2006; 32(6): 485-498.
- [18] Attard TL. Controlling all interstory displacements in highly nonlinear steel buildings using optimal viscous damping. J Struct Engrg, ASCE 2007; 133(9): 1331-1340.

- [19] Lavan O and Levy R. Optimal design of supplemental viscous dampers for irregular shear-frames in the presence of yielding. *Earthq Engrg Struct Dyn* 2005; 34(8): 889-907.
- [20] Adachi F., Yoshitomi S., Tsuji M. and Takewaki I. Nonlinear optimal oil damper design in seismically controlled multi-story building frame, *Soil Dynamics and Earthquake Engineering* 2013; 44(1), 1-13.
- [21] Tsuji M, Tanaka H, Yoshitomi S and Takewaki I. Model reduction method for buildings with viscous dampers under earthquake loading. *J Struct Construction Eng, Architectural Institute of Japan* 2011; 76(665): 1281-1290 (in Japanese).
- [22] Takewaki I and Yoshitomi S. Effects of support stiffnesses on optimal damper placement for a planar building frame. *J. of The Structural Design of Tall Buildings* 1998; 7(4): 323-336.
- [23] Noshi K, Yoshitomi S, Tsuji M and Takewaki I. Optimal nonlinear oil damper design in seismically controlled multi-story buildings for relief forces and damping coefficients, *J Structural Engineering, Architectural Institute of Japan* 2013; 59(B): 299-307 (in Japanese).
- [24] Architectural Institute of Japan (AIJ). Preliminary reconnaissance report on the 2011 Off the Pacific coast of Tohoku earthquake, April 6, 2011 (in Japanese).
- [25] Architectural Institute of Japan (AIJ). Preliminary reconnaissance report of the 2011 Tohoku-Chiho Taiheiyo-Oki earthquake, July 2011 (in Japanese).
- [26] Architectural Institute of Japan (AIJ). Preliminary reconnaissance report of the 2011 Tohoku-Chiho Taiheiyo-Oki earthquake, Springer, September 2012.
- [27] Ministry of Land, Infrastructure, Transport and Tourism (MLIT). Code draft for the retrofit of existing high-rise buildings and design guideline for new high-rise buildings, December 21, 2010 (in Japanese) (Available from http://www.mlit.go.jp/report/press/house05_hh_000218.html [Accessed on January 11, 2011]).
- [28] Takewaki I, Murakami S, Fujita K, Yoshitomi S and Tsuji M. The 2011 off the Pacific coast of Tohoku earthquake and response of high-rise buildings under long-period ground motions, *Soil Dyn. Earthq. Engrg.* 2011; **31**(11): 1511-1528.
- [29] Takewaki I, Fujita K and Yoshitomi S. Uncertainties in long-period ground motion and its impact on building structural design: Case study of the 2011 Tohoku (Japan) earthquake, *Engineering Structures* 2013; **49**: 119-134.

Captions of Tables and Figures

Table 1(a) Member properties of frame (10-story)

Table 1(b) Story stiffness and damping coefficient of oil damper (10-story)

Table 2(a) Member properties of frame (20-story)

Table 2(b) Story stiffness and damping coefficient of oil damper (20-story)

Table 3(a) Member properties of frame (40-story)

Table 3(b) Story stiffness and damping coefficient of oil damper (40-story)

Table 4(a) Member properties of frame (60-story)

Table 4(b) Story stiffness and damping coefficient of oil damper (60-story)

Table 5 Coefficients C_1, \dots, C_5 of fourth-order polynomial equation for three damper levels

Fig.1 Damping force-velocity relation of oil damper

Fig.2 Planar building model

Fig.3 Ratio of shear deformation to interstory drift in building frame with three damper levels

Fig.4 Bending deformation δ_{Rj} in interstory drift

Fig.5 Maximum horizontal damping force $f_{Lj\max}$ in linear oil damper and its approximate prediction $2h_d^{(1)}Q_{ff\max}$

Fig.6 Maximum interstory drift and maximum interstory velocity of building frame with linear oil damper

Fig.7 Absolute distribution of participation factor x interstory eigenmode of building frame without oil damper

Fig.8 Maximum horizontal damping force $f_{Lj\max}$ in linear oil damper and its approximate prediction $Z(2h_d^{(1)}Q_{ff\max})$ (El Centro NS 1940 (Lv.2))

Fig.9 Maximum horizontal damping force $f_{Lj\max}$ in linear oil damper and its approximate prediction $Y_j\{Z(2h_d^{(1)}Q_{ff\max})\}$ (El Centro NS 1940 (Lv.2))

Fig.10 Maximum horizontal damping force $f_{Lj\max}$ in linear oil damper and its approximate prediction $Y_j\{Z(2h_d^{(1)}Q_{ff\max})\}$ (Taft EW 1952 (Lv.2))

Fig.11 Maximum horizontal damping force $f_{Lj\max}$ in linear oil damper and its approximate prediction $Y_j\{Z(2h_d^{(1)}Q_{ff\max})\}$ (Hachinohe NS 1968 (Lv.2))

Fig.12 Maximum horizontal damping force $f_{Lj\max}$ in linear oil damper and its approximate predictions $Y_j\{Z(2h_d^{(1)}Q_{ff\max})\}$ and $Y_j\{Z^*(2h_d^{(1)}Q_{ff\max})\}$ (Hachinohe NS 1968 (Lv.2))

Fig.13 Flowchart for evaluation of relief force of oil damper

Fig.A1 (a) Participation vector, (b) Absolute value of interstory drift participation vector

Table 1(a) Member properties of frame (10-story)

Story no.	$I_b(\text{mm}^4)$	$I_c(\text{mm}^4)$	$A_c(\text{mm}^2)$
1~5	2.92×10^9	2.16×10^9	46464
6~10	1.72×10^9	1.90×10^9	40356

Table 1(b) Story stiffness and damping coefficient of oil damper (10-story)

Story no.	$k_{\bar{f}j}$ (kN/mm)	$c_{1j,2}(\text{kN} \cdot \text{s/mm})$		
		$h_d^{(1)} = 5\%$	$h_d^{(1)} = 10\%$	$h_d^{(1)} = 15\%$
1	182	4.64	9.27	13.9
2	119	3.05	6.10	9.15
3	113	2.89	5.77	8.66
4	110	2.82	5.63	8.45
5	106	2.72	5.44	8.16
6	87.7	2.24	4.48	6.72
7	75.0	1.91	3.83	5.74
8	71.0	1.81	3.63	5.44
9	66.6	1.70	3.40	5.10
10	54.0	1.38	2.76	4.14

Table 2(a) Member properties of frame (20-story)

Story no.	$I_b(\text{mm}^4)$	$I_c(\text{mm}^4)$	$A_c(\text{mm}^2)$
1~5	4.11×10^9	7.04×10^9	80864
6~10	2.92×10^9	3.64×10^9	55264
11~15	2.92×10^9	2.16×10^9	46464
16~20	1.72×10^9	1.90×10^9	40356

Table 2(b) Story stiffness and damping coefficient of oil damper (20-story)

Story no.	$k_{\bar{f}j}$ (kN/mm)	$c_{1j,2}(\text{kN} \cdot \text{s/mm})$		
		$h_d^{(1)} = 5\%$	$h_d^{(1)} = 10\%$	$h_d^{(1)} = 15\%$
1	396	18.1	36.1	54.2
2	220	10.0	20.1	30.1
3	195	8.88	17.8	26.6
4	184	8.41	16.8	25.2
5	175	7.98	16.0	23.9
6	134	6.13	12.3	18.4
7	119	5.45	10.9	16.3
8	114	5.22	10.4	15.7
9	111	5.07	10.1	15.2
10	108	4.91	9.82	14.7
11	92.1	4.21	8.41	12.6
12	89.2	4.07	8.14	12.2
13	86.2	3.94	7.87	11.8
14	82.8	3.78	7.56	11.3
15	78.2	3.57	7.13	10.7
16	65.0	2.97	5.93	8.90
17	54.8	2.50	5.00	7.51
18	48.8	2.23	4.45	6.68
19	40.8	1.86	3.73	5.59
20	26.9	1.23	2.45	3.68

Table 3(a) Member properties of frame (40-story)

Story no.	$I_b(\text{mm}^4)$	$I_c(\text{mm}^4)$	$A_c(\text{mm}^2)$
1~10	6.94×10^9	26.2×10^9	171900
11~20	3.91×10^9	21.0×10^9	135100
21~30	3.23×10^9	7.77×10^9	77500
31~40	3.23×10^9	2.60×10^9	46400

Table 3(b) Story stiffness and damping coefficient of oil damper (40-story)

Story no.	k_{fi} (kN/mm)	$c_{1j,3}(\text{kN} \cdot \text{s/mm})$		
		$h_d^{(1)} = 5\%$	$h_d^{(1)} = 10\%$	$h_d^{(1)} = 15\%$
1	1442	105	210	316
2	707	51.6	103	155
3	592	43.2	86.4	130
4	552	40.2	80.5	121
5	531	38.7	77.4	116
6	516	37.6	75.2	113
7	503	36.7	73.3	110
8	489	35.7	71.4	107
9	472	34.4	68.9	103
10	443	32.3	64.6	96.8
11	371	27.0	54.0	81.1
12	319	23.2	46.5	69.7
13	299	21.8	43.6	65.5
14	290	21.1	42.3	63.4
15	284	20.7	41.4	62.1
16	279	20.4	40.7	61.1
17	275	20.1	40.1	60.2
18	271	19.8	39.5	59.3
19	266	19.4	38.8	58.2
20	259	18.9	37.8	56.7
21	223	16.3	32.6	48.8
22	209	15.3	30.5	45.8
23	203	14.8	29.7	44.5
24	199	14.5	29.1	43.6
25	196	14.3	28.6	42.8
26	192	14.0	28.0	42.0
27	188	13.7	27.5	41.2
28	184	13.4	26.9	40.3
29	180	13.1	26.2	39.3
30	174	12.7	25.3	38.0
31	141	10.3	20.5	30.8
32	136	9.93	19.9	29.8
33	131	9.57	19.1	28.7
34	125	9.14	18.3	27.4
35	118	8.62	17.2	25.9
36	110	8.00	16.0	24.0
37	98.9	7.21	14.4	21.6
38	85.0	6.20	12.4	18.6
39	66.3	4.83	9.66	14.5
40	39.3	2.87	5.73	8.60

Table 4(a) Member properties of frame (60-story)

Story no.	$I_b(\text{mm}^4)$	$I_c(\text{mm}^4)$	$A_c(\text{mm}^2)$
1~10	12.5×10^9	50.8×10^9	230000
11~20	5.62×10^9	28.7×10^9	190000
21~30	4.40×10^9	17.0×10^9	137600
31~40	2.96×10^9	9.14×10^9	92400
41~50	2.96×10^9	5.13×10^9	67500
51~60	2.96×10^9	5.13×10^9	67500

Table 4(b) Story stiffness and damping coefficient of oil damper (60-story)

Story no.	k_{fj} (kN/mm)	$c_{1j,3}$ (kN · s/mm)		
		$h_d^{(1)} = 5\%$	$h_d^{(1)} = 10\%$	$h_d^{(1)} = 15\%$
1	2349	221	441	662
2	1101	103	207	310
3	895.2	84.1	168	252
4	819.9	77.0	154	231
5	780.6	73.3	147	220
6	753.4	70.7	141	212
7	730.1	68.6	137	206
8	705.6	66.2	132	199
9	673.6	63.2	126	190
10	622.4	58.4	117	175
11	481.4	45.2	90.4	136
12	392.3	36.8	73.7	110
13	361.0	33.9	67.8	102
14	346.7	32.6	65.1	97.7
15	338.7	31.8	63.6	95.4
16	333.1	31.3	62.6	93.8
17	328.4	30.8	61.7	92.5
18	323.5	30.4	60.8	91.1
19	317.6	29.8	59.6	89.5
20	308.7	29.0	58.0	87.0
21	279.4	26.2	52.5	78.7
22	260.4	24.5	48.9	73.4
23	252.2	23.7	47.4	71.1
24	247.7	23.3	46.5	69.8
25	244.4	22.9	45.9	68.8
26	241.6	22.7	45.4	68.0
27	238.7	22.4	44.8	67.2
28	235.4	22.1	44.2	66.3
29	230.8	21.7	43.3	65.0
30	222.7	20.9	41.8	62.7
31	191.2	18.0	35.9	53.9
32	172.0	16.2	32.3	48.5
33	165.2	15.5	31.0	46.5
34	161.9	15.2	30.4	45.6
35	159.7	15.0	30.0	45.0
36	157.8	14.8	29.6	44.5
37	156.1	14.7	29.3	44.0
38	154.3	14.5	29.0	43.5
39	152.3	14.3	28.6	42.9
40	150.0	14.1	28.2	42.3
41	140.0	13.1	26.3	39.4
42	138.1	13.0	25.9	38.9
43	136.0	12.8	25.5	38.3
44	133.8	12.6	25.1	37.7
45	131.4	12.3	24.7	37.0
46	128.9	12.1	24.2	36.3
47	126.1	11.8	23.7	35.5
48	123.1	11.6	23.1	34.7
49	119.8	11.2	22.5	33.7
50	116.1	10.9	21.8	32.7
51	112.0	10.5	21.0	31.6
52	107.4	10.1	20.2	30.3
53	102.2	9.59	19.2	28.8
54	96.16	9.03	18.1	27.1
55	89.15	8.37	16.7	25.1
56	80.88	7.59	15.2	22.8
57	70.99	6.67	13.3	20.0
58	58.92	5.53	11.1	16.6
59	43.83	4.12	8.23	12.3
60	24.39	2.29	4.58	6.87

Table 5 Coefficients C_1, \dots, C_5 of fourth-order polynomial equation for three damper levels

(a)20-story frame

$h_d^{(1)} \backslash$	C_1	C_2	C_3	C_4	C_5
5%	0.000	-0.001	0.032	-0.249	1.554
10%	0.000	-0.001	0.033	-0.316	1.747
15%	0.000	-0.001	0.045	-0.412	2.074

(b)40-story frame

$h_d^{(1)} \backslash$	C_1	C_2	C_3	C_4	C_5
5%	0.000	-0.001	0.033	-0.498	4.770
10%	0.000	-0.002	0.050	-0.579	4.056
15%	0.000	-0.002	0.055	-0.563	3.467

(c)60-story frame

$h_d^{(1)} \backslash$	C_1	C_2	C_3	C_4	C_5
5%	0.000	-0.001	0.042	-0.723	6.056
10%	0.000	-0.001	0.046	-0.652	4.561
15%	0.000	-0.001	0.040	-0.540	3.576

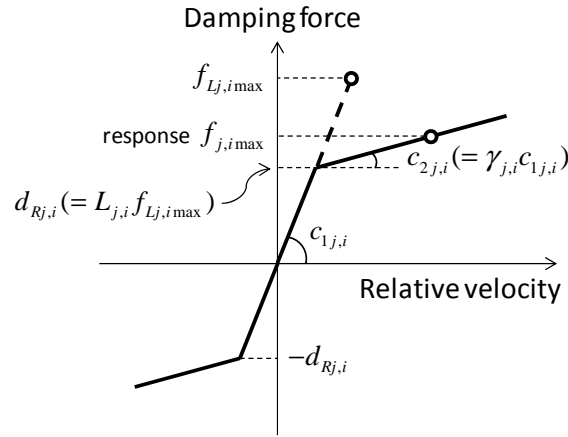


Fig.1 Damping force-velocity relation of oil damper

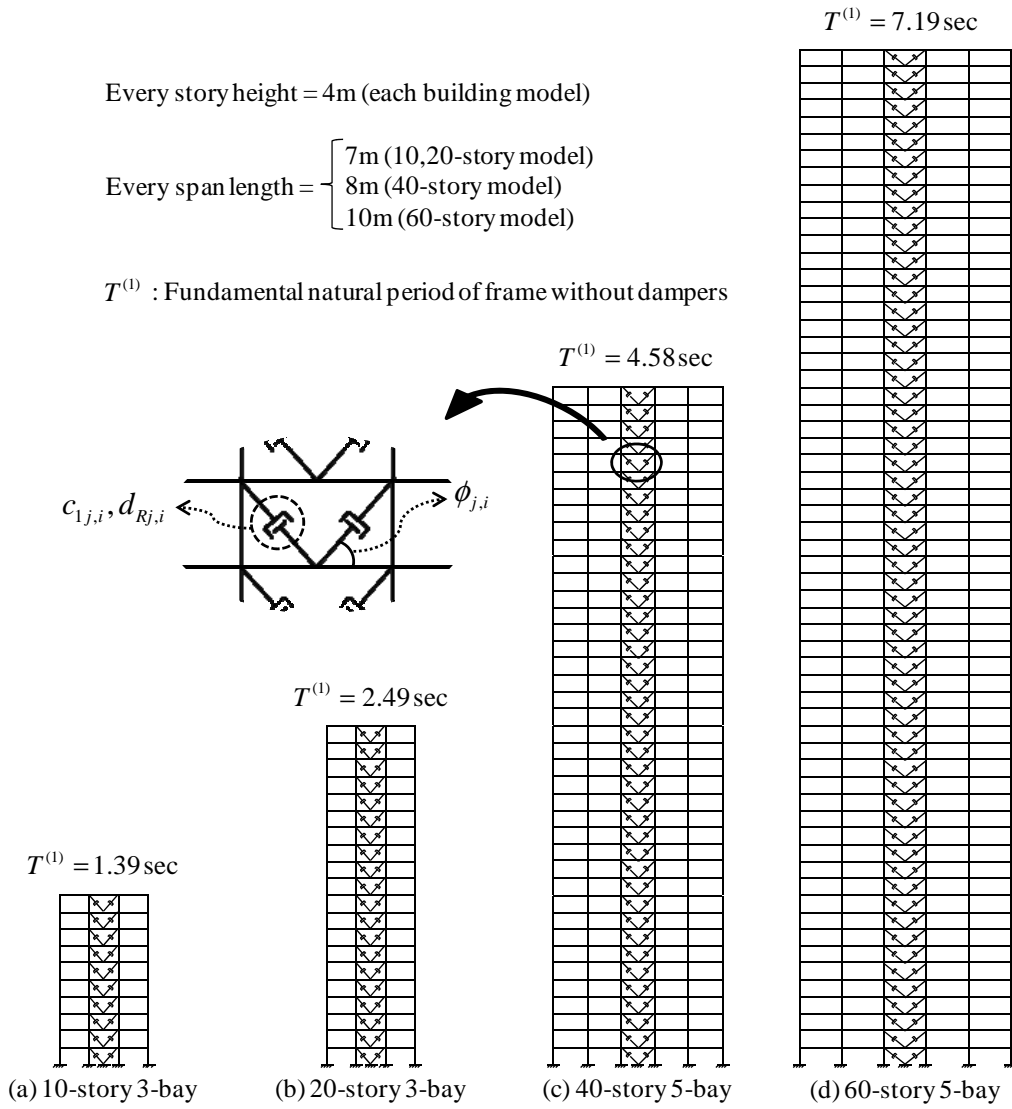
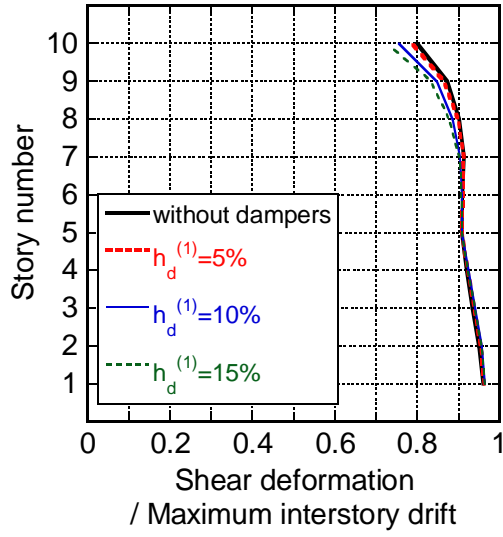
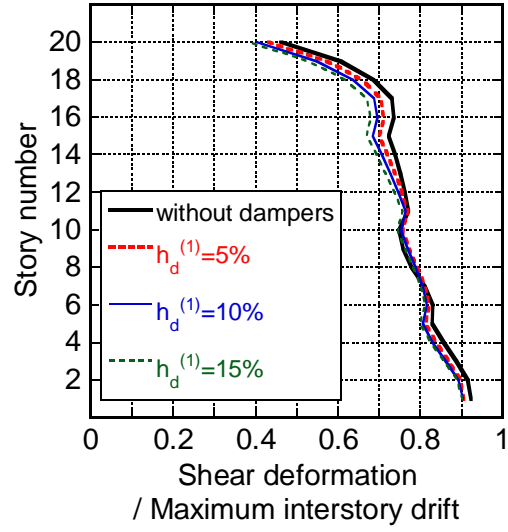


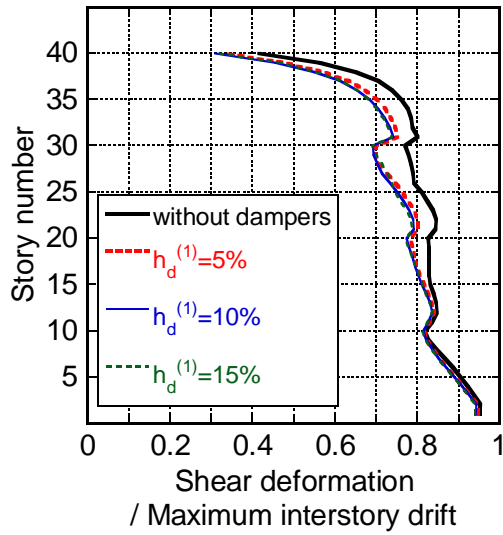
Fig.2 Planar building model



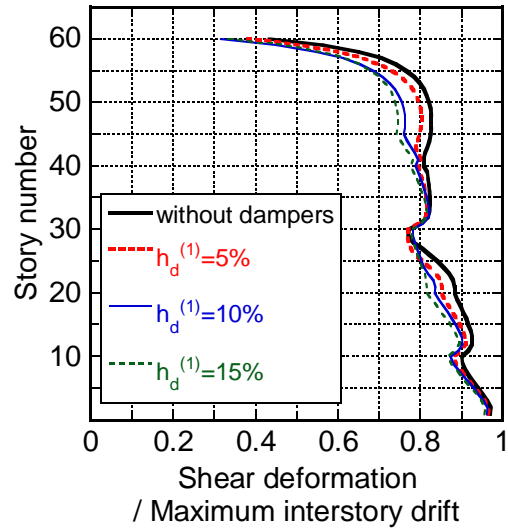
(a) 10-story 3-bay building model



(b) 20-story 3-bay building model



(c) 40-story 5-bay building model



(d) 60-story 5-bay building model

Fig.3 Ratio of shear deformation to interstory drift in building frame with three damper levels

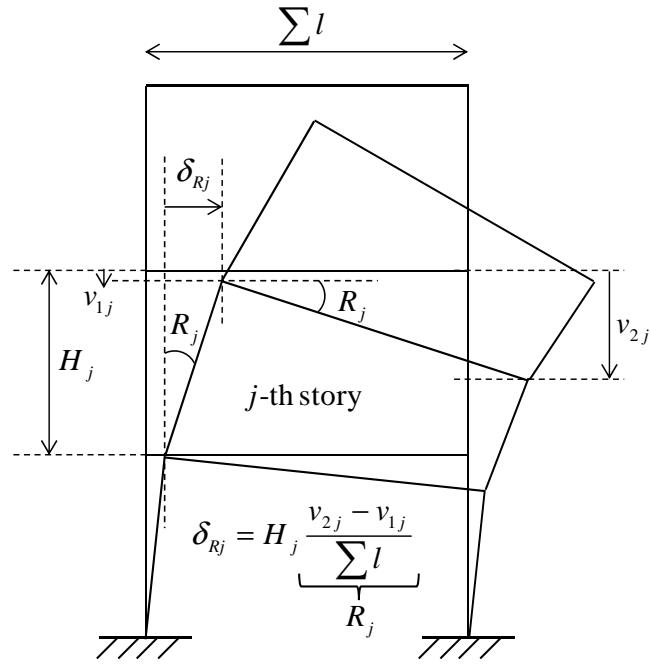
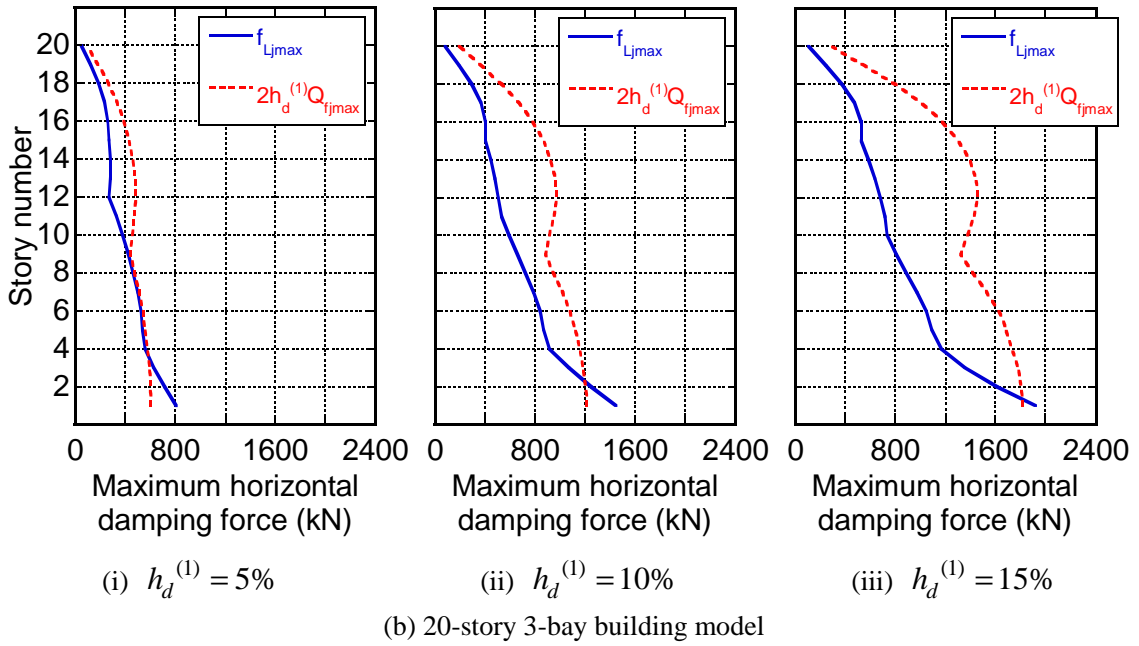
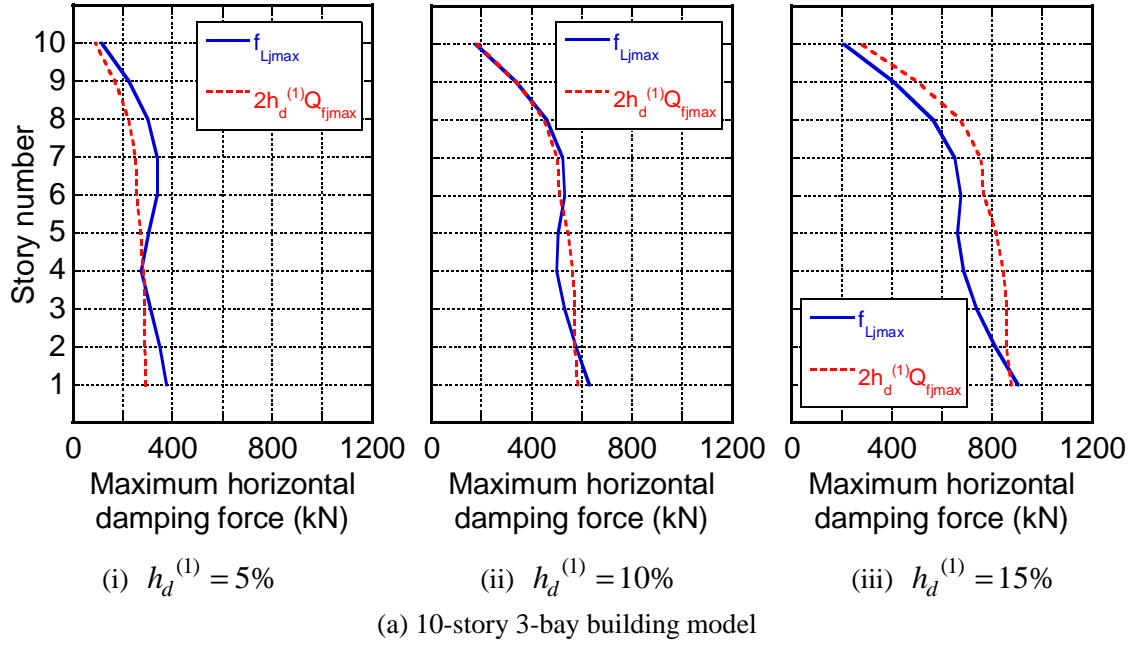


Fig.4 Bending deformation δ_{Rj} in interstory drift



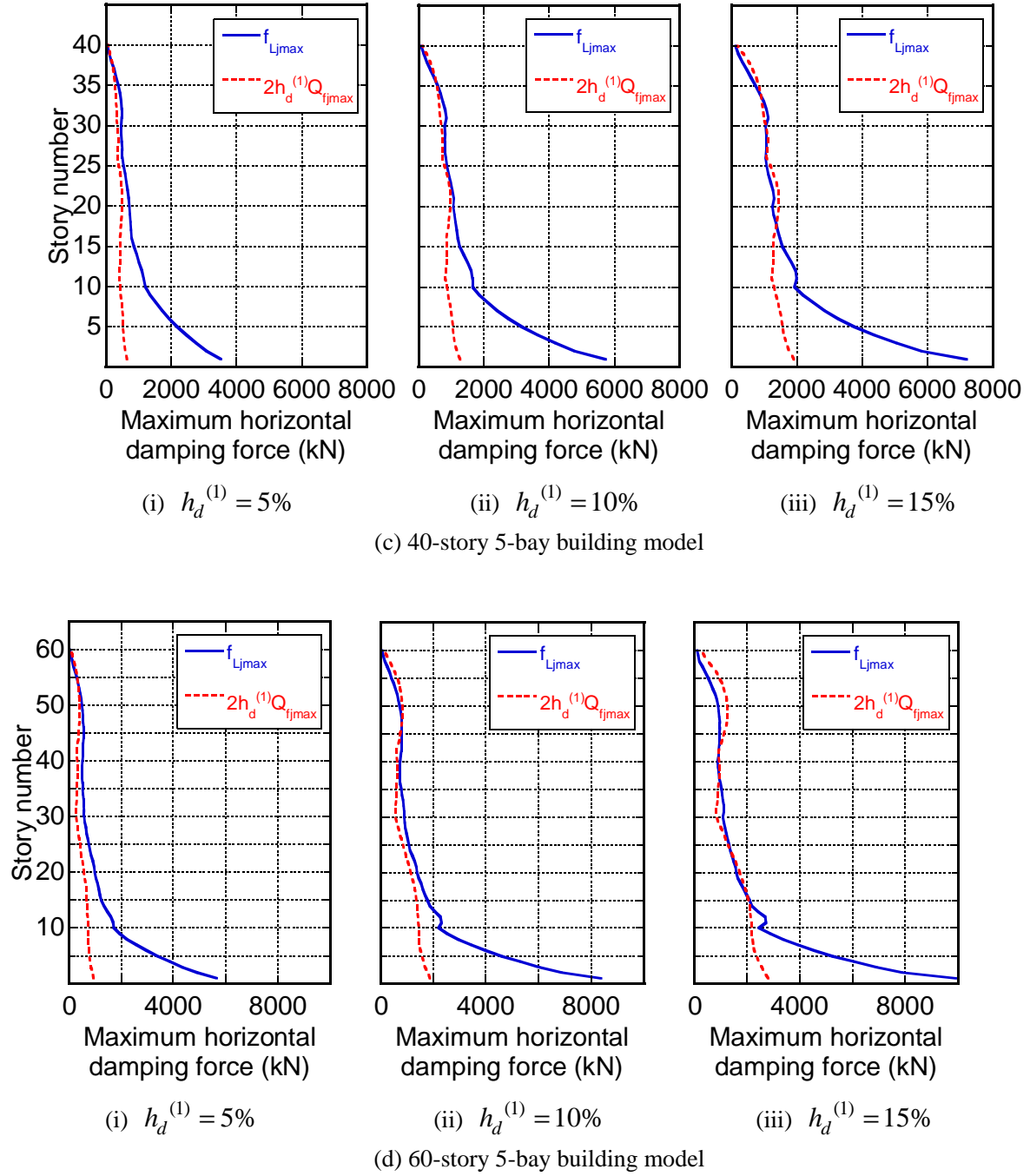
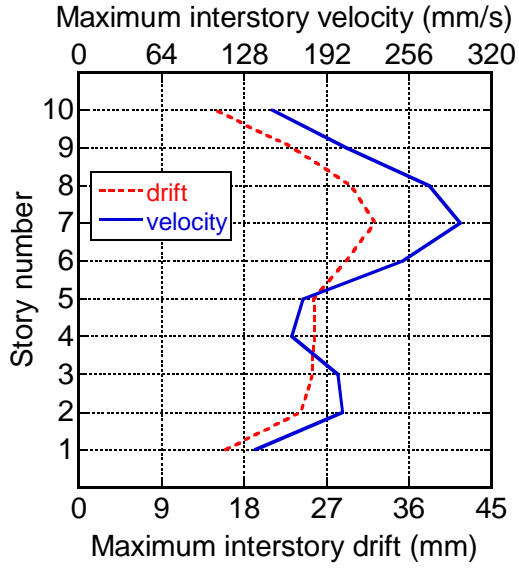
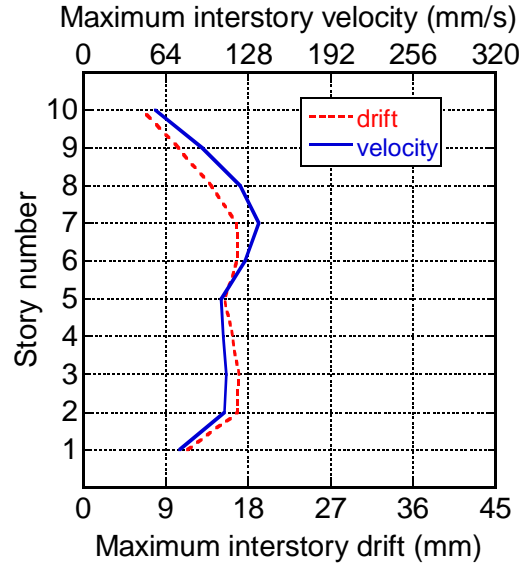


Fig.5 Maximum horizontal damping force $f_{Lj\max}$ in linear oil damper and its approximate prediction $2h_d^{(1)}Q_{fj\max}$

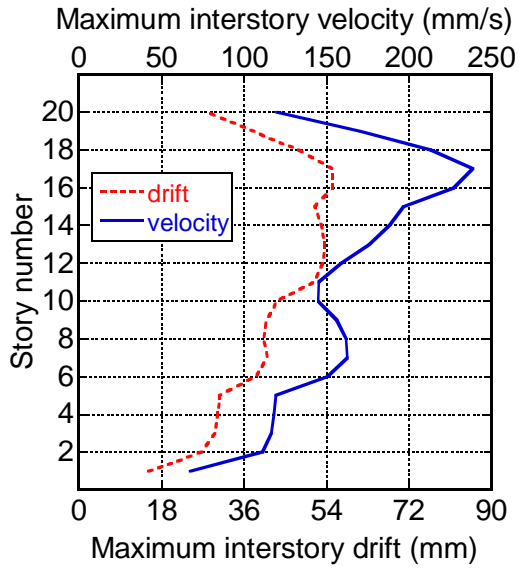


(i) without dampers

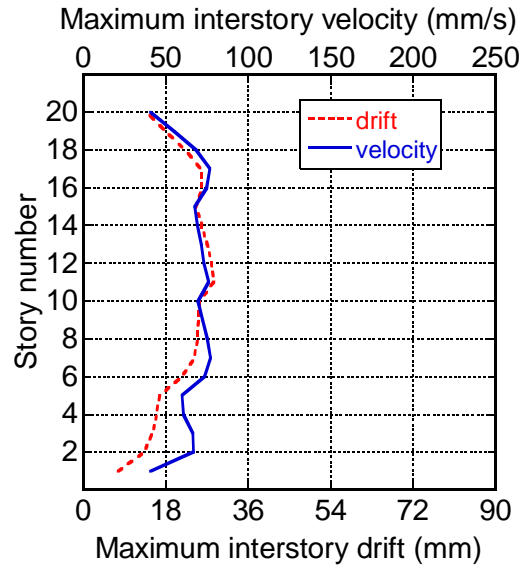


(ii) $h_d^{(1)} = 15\%$

(a) 10-story 3-bay building model



(i) without dampers



(ii) $h_d^{(1)} = 15\%$

(b) 20-story 3-bay building model

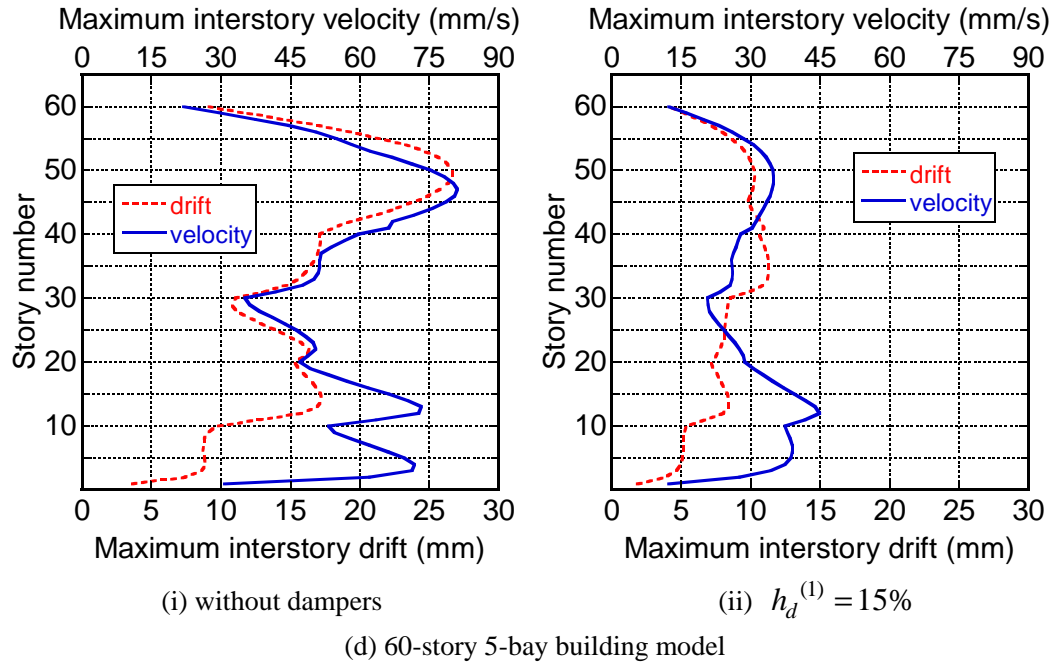
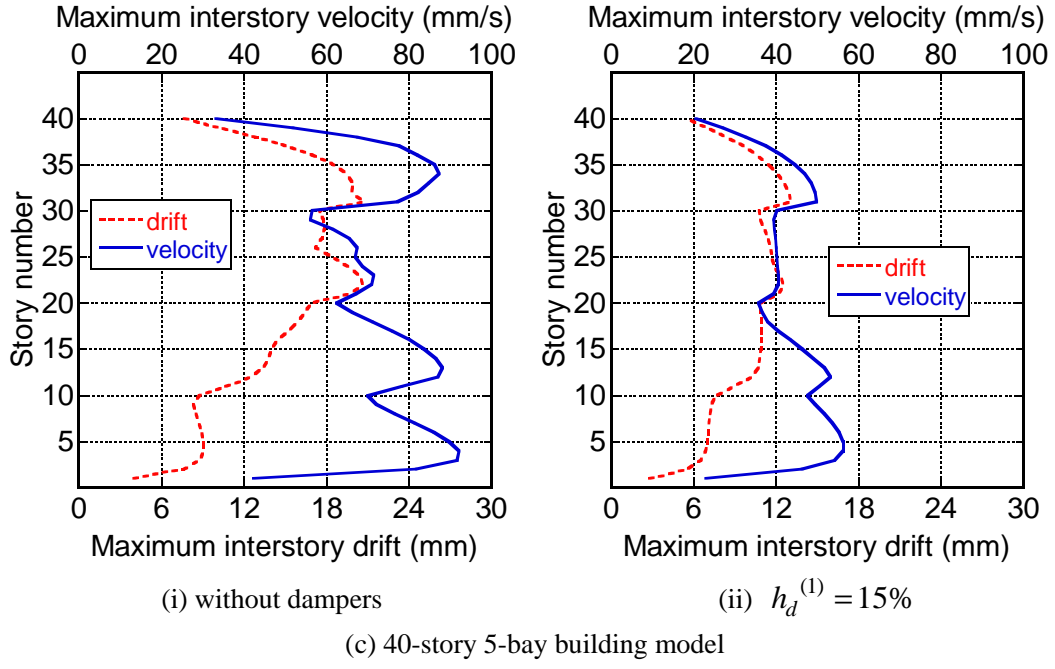


Fig.6 Maximum interstory drift and maximum interstory velocity of building frame with linear oil damper

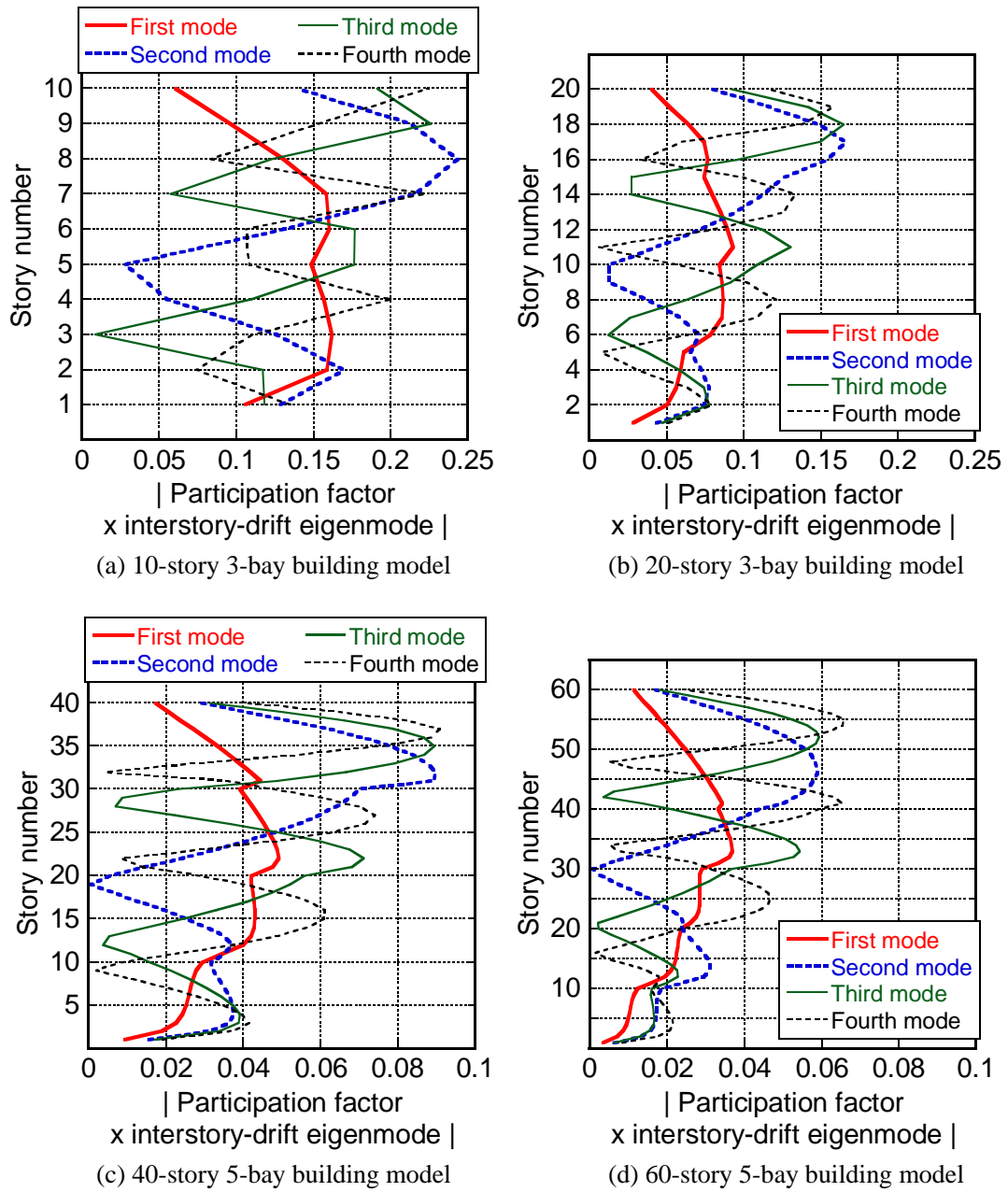
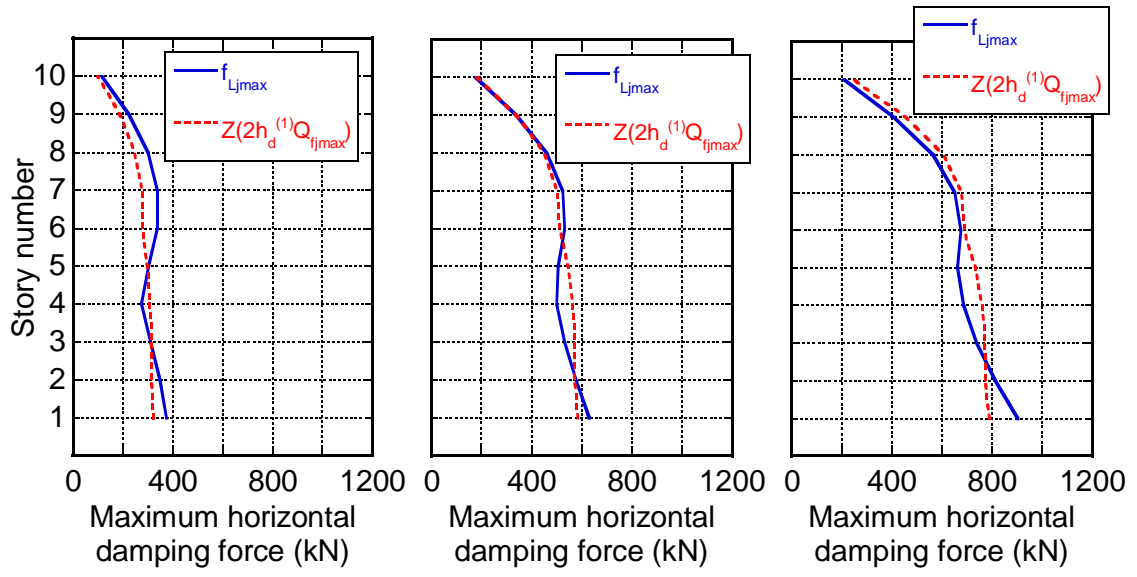
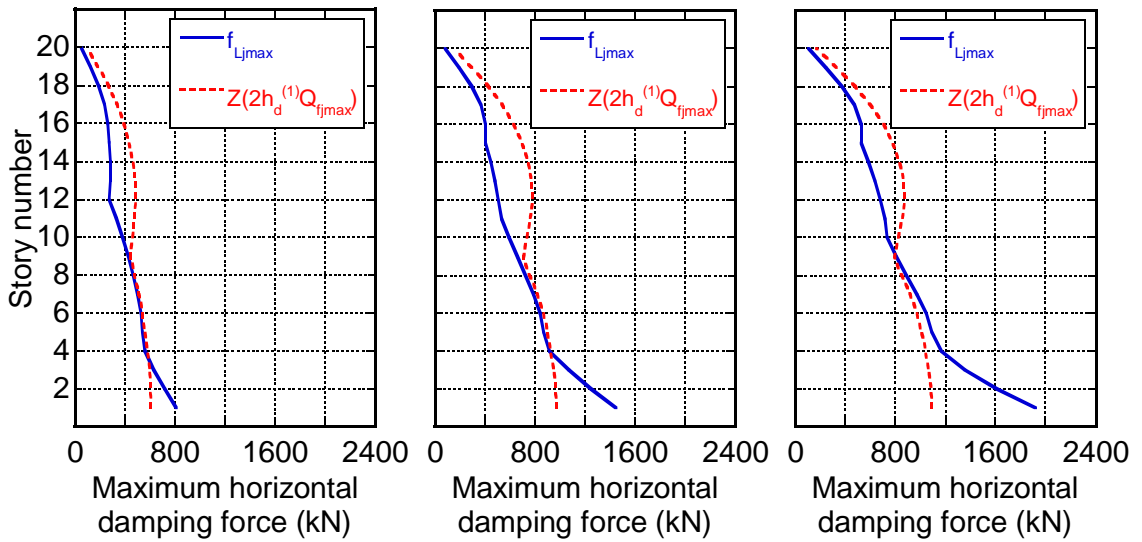


Fig.7 Absolute distribution of participation factor x interstory eigenmode of building frame without oil damper

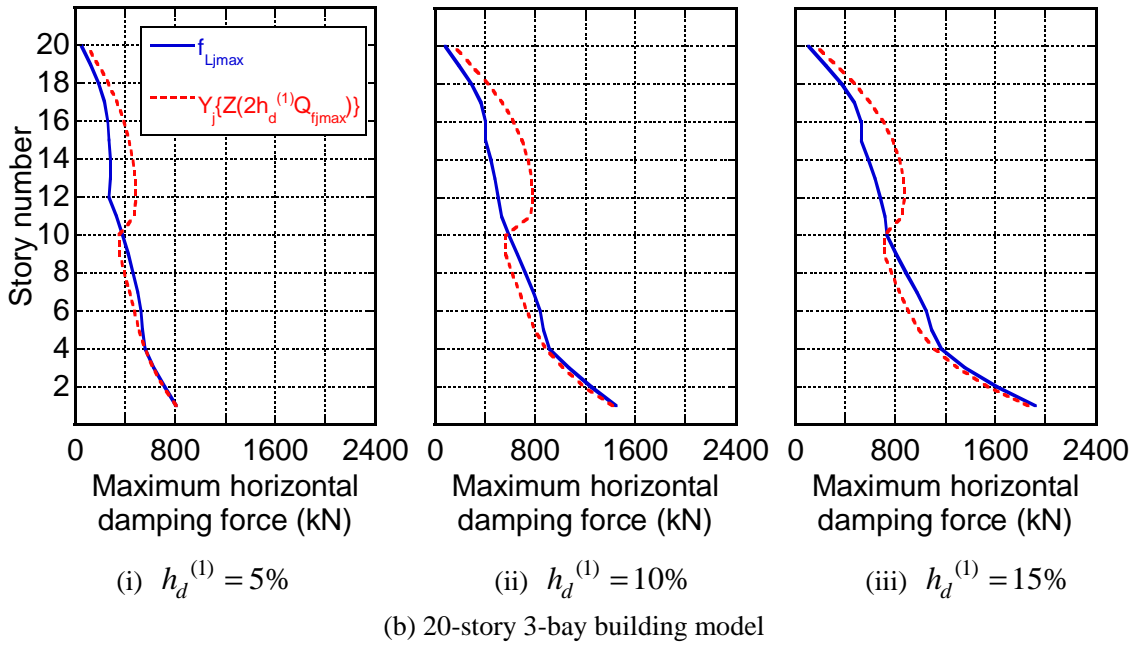
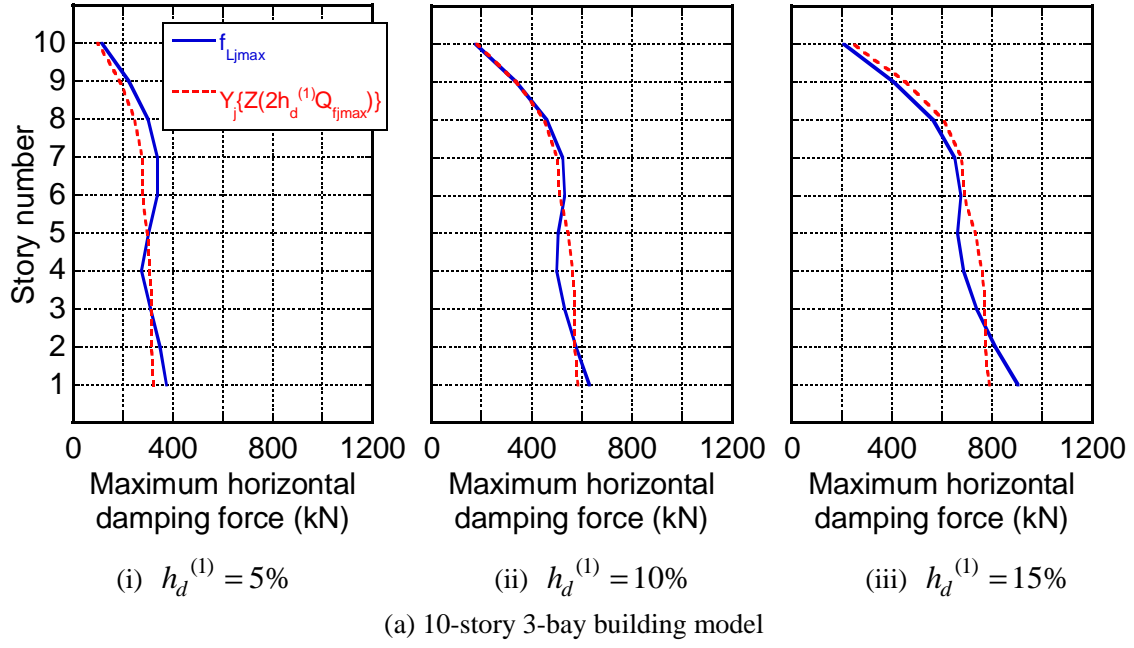


(a) 10-story 3-bay building model



(b) 20-story 3-bay building model

Fig.8 Maximum horizontal damping force $f_{Lj\max}$ in linear oil damper and its approximate prediction $Z(2h_d^{(1)}Q_{fj\max})$ (El Centro NS 1940 (Lv.2))



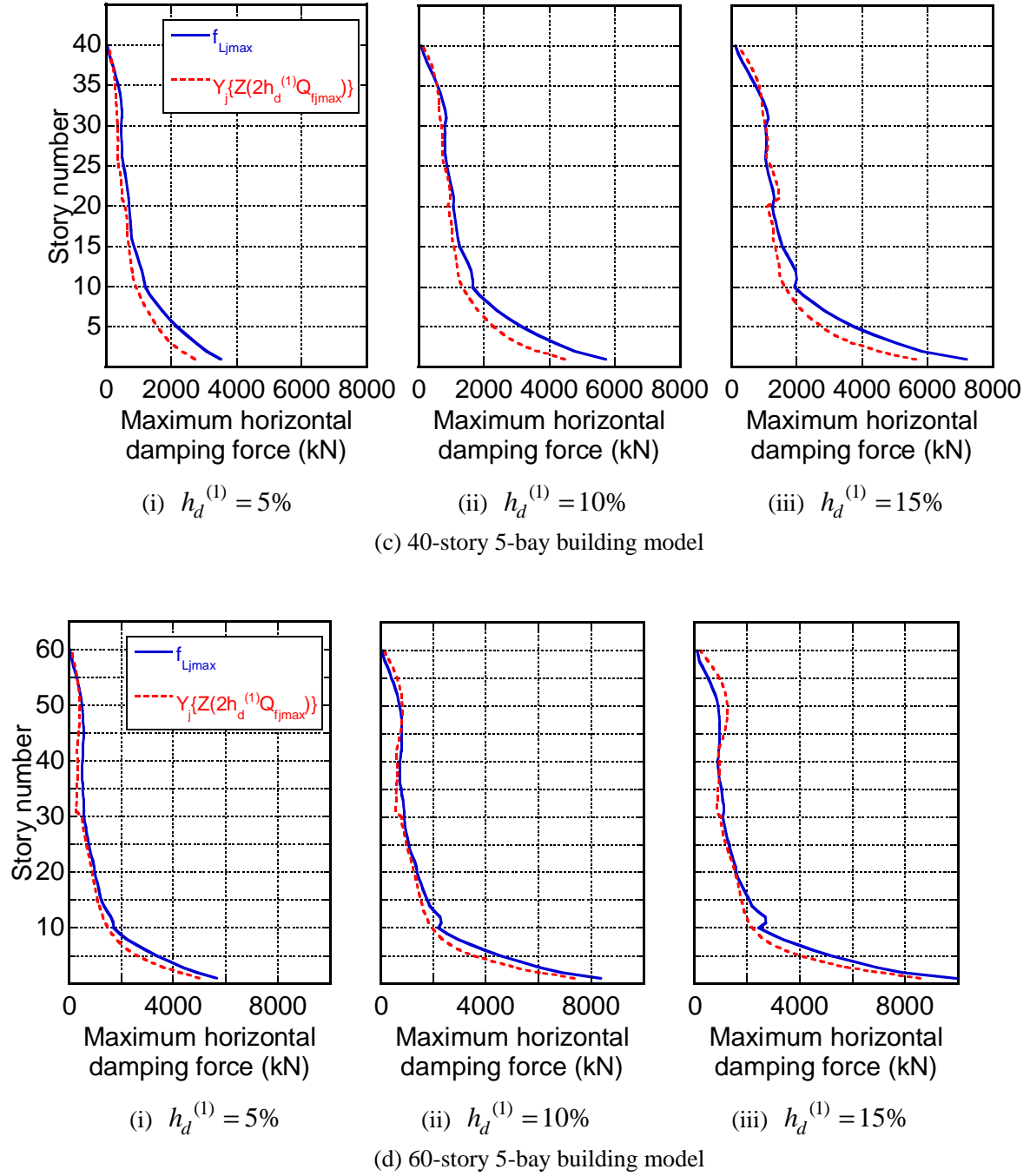
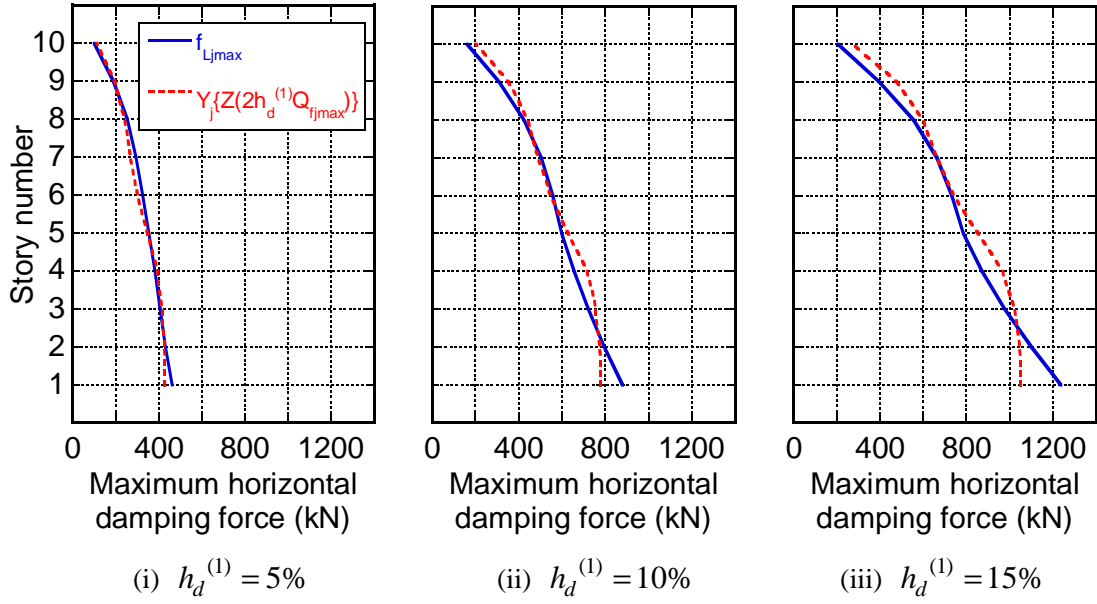
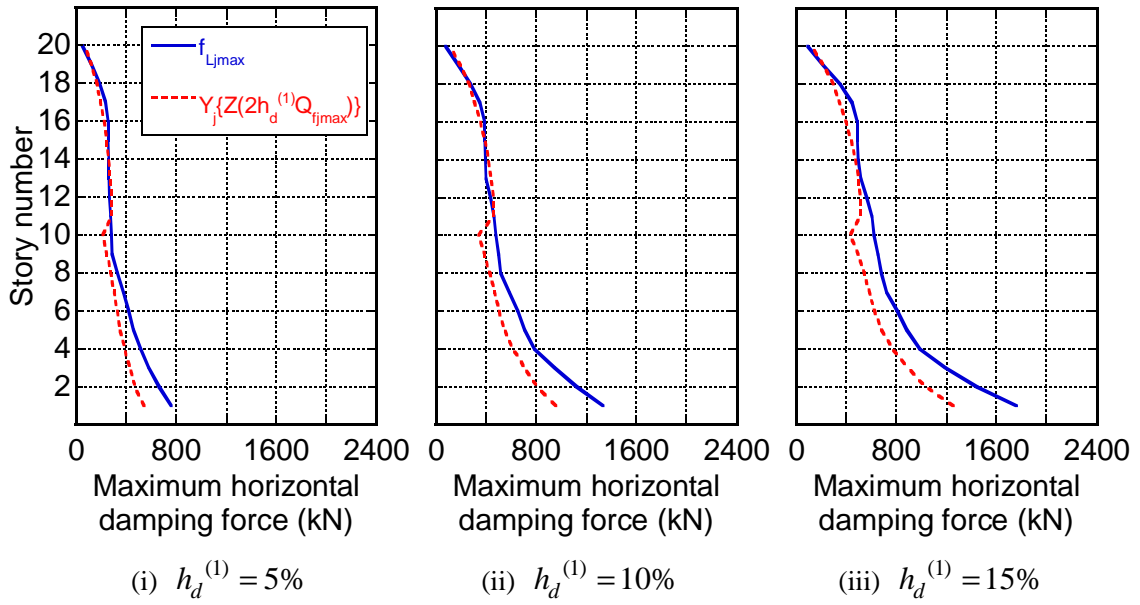


Fig.9 Maximum horizontal damping force $f_{Lj\max}$ in linear oil damper and its approximate prediction $Y_j\{Z(2h_d^{(1)}Q_{fj\max})\}$ (El Centro NS 1940 (Lv.2))



(a) 10-story 3-bay building model



(b) 20-story 3-bay building model

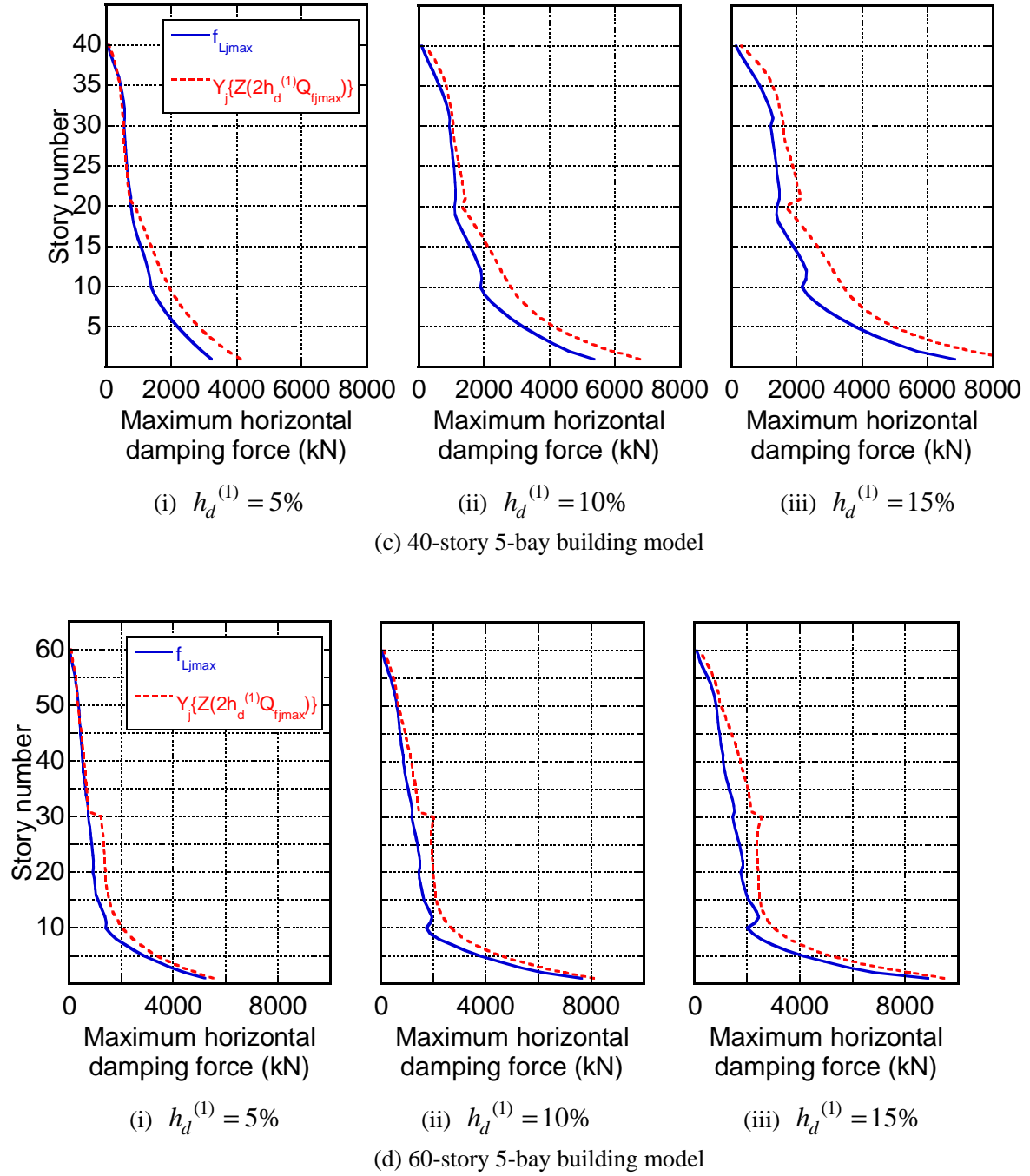
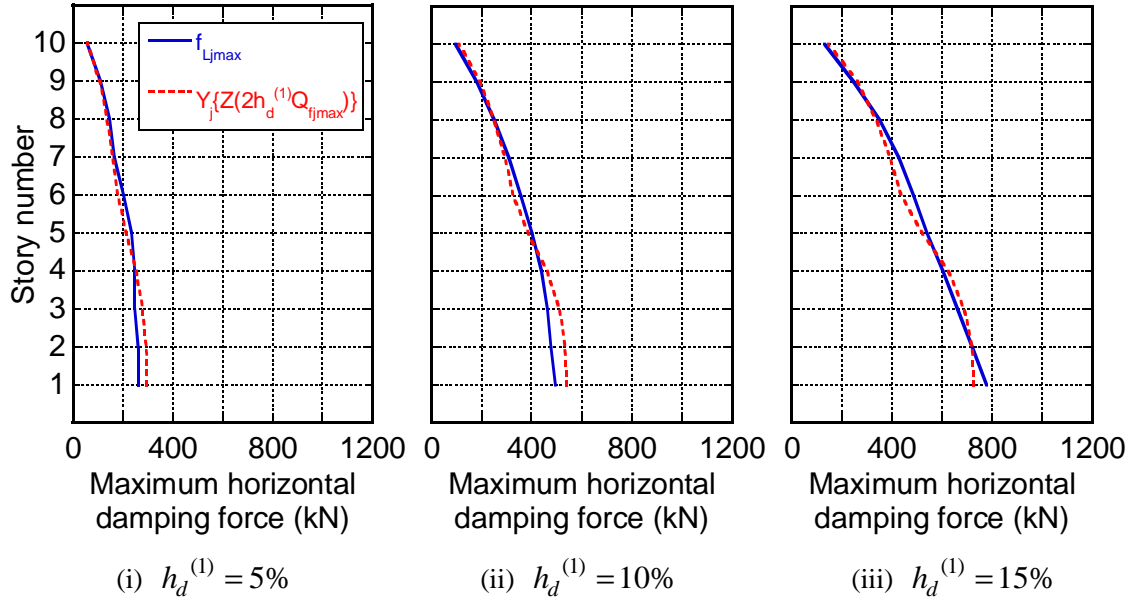
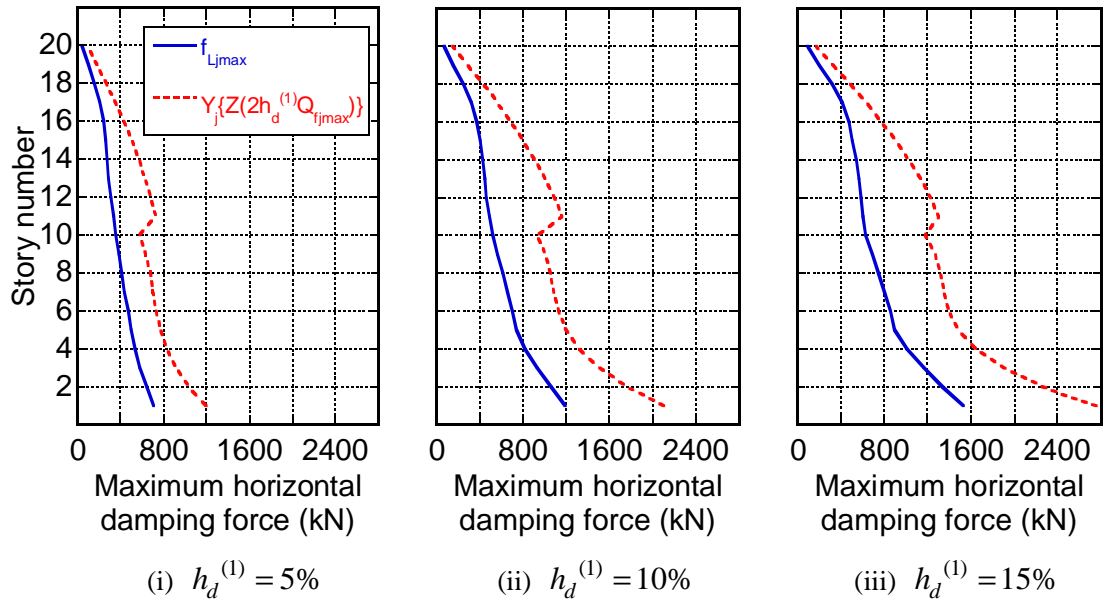


Fig.10 Maximum horizontal damping force f_{Ljmax} in linear oil damper and its approximate prediction $Y_j\{Z(2h_d^{(1)}Q_{fjmax})\}$ (Taft EW 1952 (Lv.2))



(a) 10-story 3-bay building model



(b) 20-story 3-bay building model

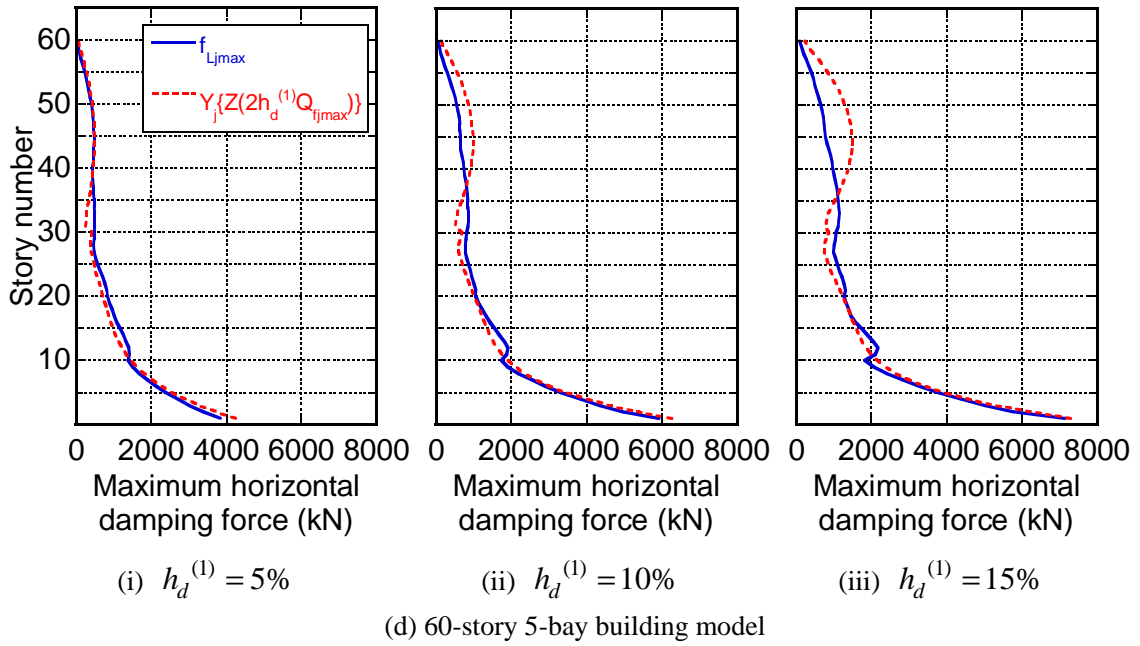
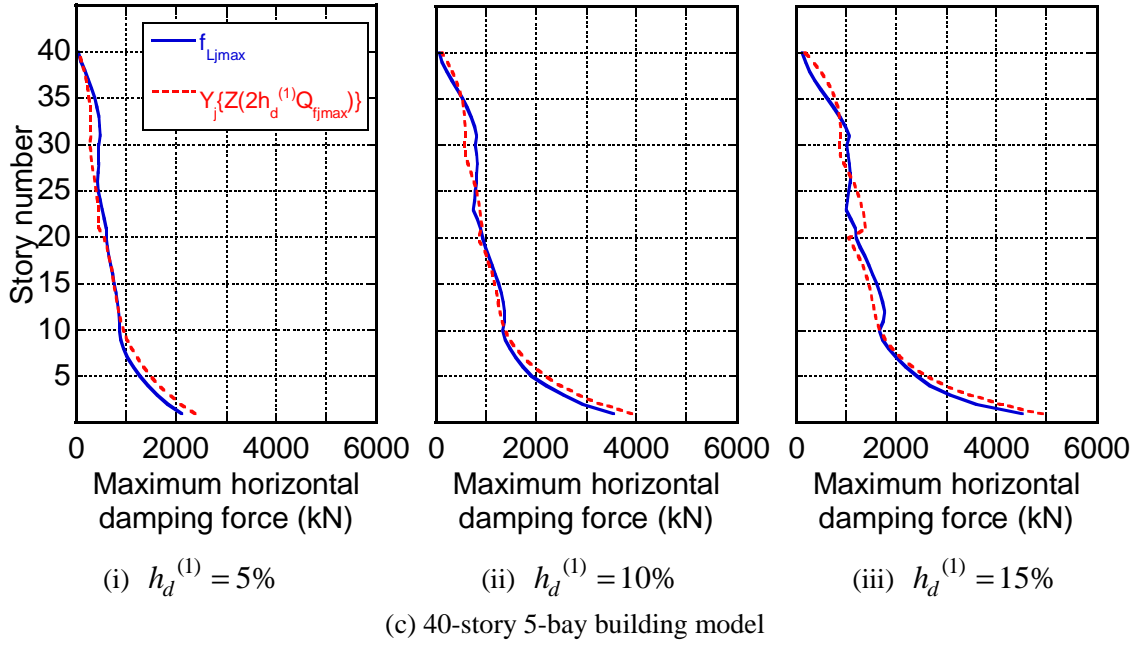


Fig.11 Maximum horizontal damping force $f_{Lj\max}$ in linear oil damper and its approximate prediction $Y_j\{Z(2h_d^{(1)}Q_{ffj\max})\}$ (Hachinohe NS 1968 (Lv.2))

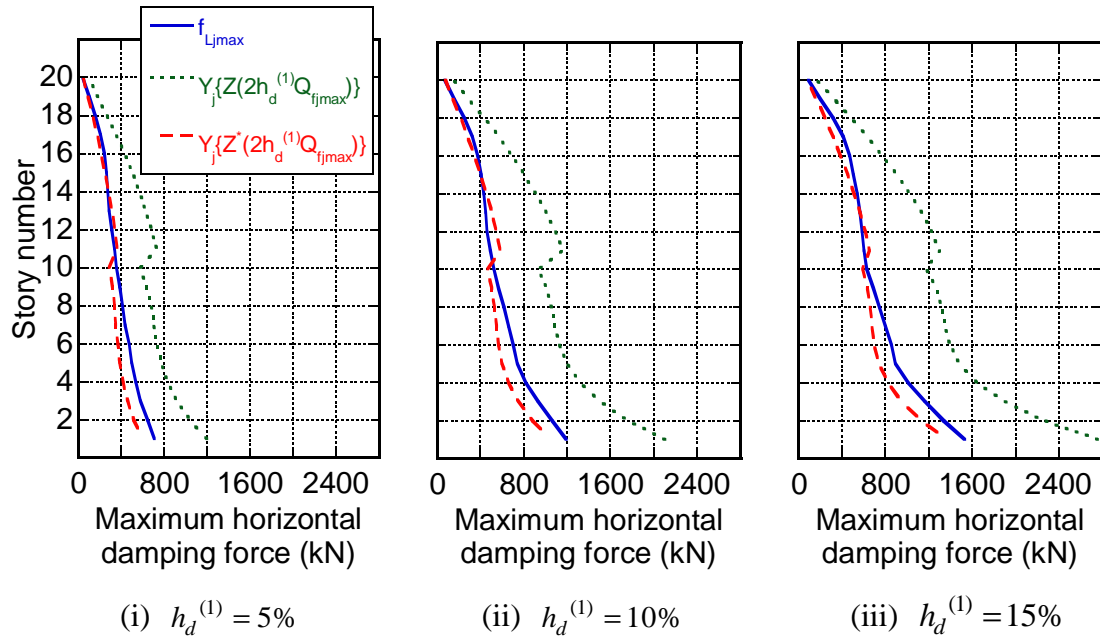


Fig.12 Maximum horizontal damping force $f_{Lj\max}$ in linear oil damper and its approximate predictions $Y_j\{Z(2h_d^{(1)}Q_{ff\max})\}$ and $Y_j\{Z^*(2h_d^{(1)}Q_{ff\max})\}$ (Hachinohe NS 1968 (Lv.2))

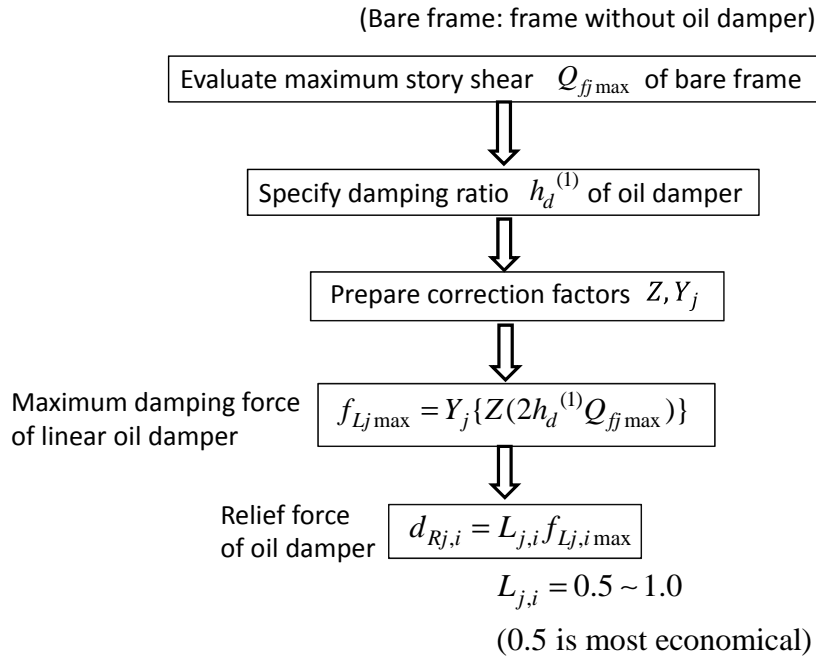


Fig.13 Flowchart for evaluation of relief force of oil damper

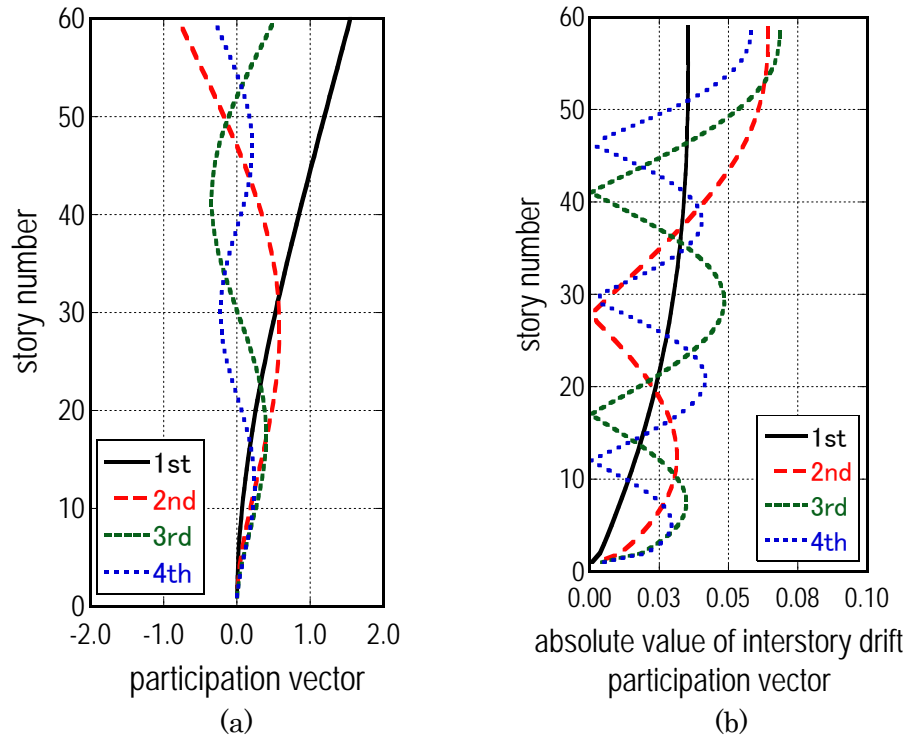


Fig.A1 (a) Participation vector, (b) Absolute value of interstory drift participation vector